

Virtual Reassembly of Fractured Bones for Orthopedic Surgery

Wang, Lei*

Beihang University

Pan, Junjun[†]

Beihang University

Yao, Qingqiang[‡]

Nanjing First Hospital,

Nanjing Medical University

ABSTRACT

In orthopedic surgery, the traditional restoration of comminuted fracture basically relies on surgeon's manual work, which is usually intricate and error-prone. If fractured bones are poorly reassembled, the patient may suffer from more exposure to radiation and longer recovery time. More severely, some operation mistakes can cause sequela, such as joint dysfunction and infection. Therefore, orthopedic surgeons urgently need an intelligent assistance solution to improve the accuracy and reliability of fractured bones reassembly in procedure. This paper presents an automatic pipeline for virtual reassembly of fractured bones which are broken into pieces. It uses an intact bone as a template. We first reconstruct the 3D fractured bone from CT data using MIMICS. Then we analyze the shape structure of bone model through extracting key feature points and comparing descriptors. Finally, we search the correspondence between the fragments and template. The aligning is performed to ensure the fragments can join together. Compared with some semi-automatic reassembly methods for archaeological artifacts and forensic evidences, ours is fully automatic without human interactions and specialized to medical purposes. It can help orthopedic surgeons to make correct decisions in fractured bones reassembly.

Keywords: Fractured bone, reassembly, keypoints, descriptor, template

1 INTRODUCTION

Comminuted fracture repairing surgery (Figure 1) is an effective treatment for patients who break their bones into pieces. In the procedure, surgeons should find the similarity between every piece and put them back on the original place,

which is a complicated and time-consuming task. Traditionally, since surgeons cannot see the inside environment intuitively before splitting the soft tissue and reveal the fractured bones, they

can only refer to their clinical experience to find correspondence among the pieces with the help of X-ray or CT images. However, subjective judgement unavoidably makes mistakes and causes

inaccurate matching, which will make the patient endure longer recovery time. Major misplacements can lead to postoperative complications and even failure of surgery. Additionally, in traditional procedure, the surgery usually takes very long time and patients need being exposed to more radiation.

With the advance of medical imaging and computer assisted surgery technology, there emerges some new alternatives. CT scans the human body and obtains high-resolution 3D geometry information that precisely depict details of each bone. The geometry data can be adopted to reconstruct bone models, with which we can create a virtual platform and operate on computers to simulate the real surgery. Furthermore, as the models maintain both geometry structure of each bone and details of the broken faces, we can process and analyze their feature to perform automatic matching of the fractured bones. When all pieces combining together, it is possible to achieve reassembling the bones beforehand.

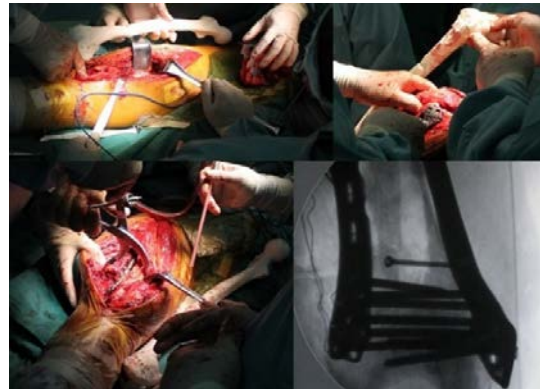


Figure 1: Comminuted fracture repairing surgery

*e-mail: wang3s@foxmail.com

[†]e-mail: pan_junjun@buaa.edu.cn

[‡]e-mail: yaoqingqiang@gmail.com

Reassembling the fractured pieces on computer before a surgery offers great help. It can provide a platform for surgeons to virtually rehearse the surgery and give them more reference to assess complexity and anticipate potential difficulty in three-dimensional space. In this paper, we develop an effective pipeline to create 3D model of broken bone pieces from CT image and reassemble them virtually without any manual help. Moreover, we analyze and compare the commonly used keypoints detector and descriptor for 3D model processing, tracking and registration. We mainly adopt template-based assembling methods, which needs a complete bone model as a template and align the fragment onto the template so that they can patch together. Our work mainly consists of three steps, which can be illustrated as Figure 2:

- 1) Creating 3D model of pieces and template from CT images;
- 2) Extracting keypoints on each model and calculate

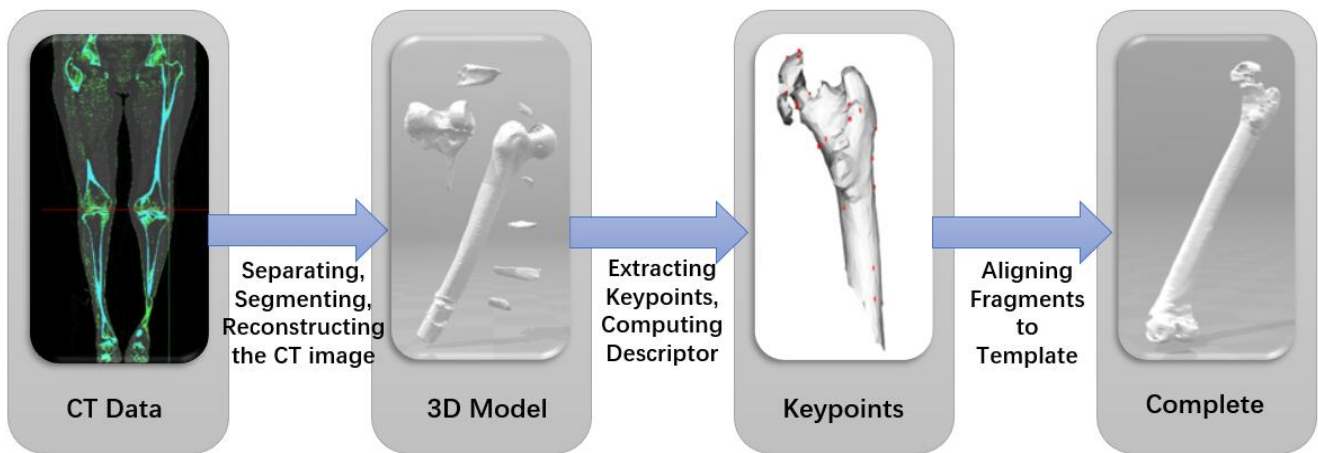


Figure 2: Flowchart of our method

- 3) Performing a template matching to align the pieces and template.

The main contributions of our work include:

- 1) We propose a complete pipeline to virtually reassemble fractured bones including reconstructing model, extracting keypoints and computing descriptor and aligning fragments to template.
- 2) We develop a system to implement the reassembly method. It can be applied in comminuted fracture repairing surgery and help surgeons in the real medical situations.
- 3) Compared with the general reassembly pipeline, our method is specially designed for orthopedic surgery which covers both CT data preprocessing and subsequent matching operations.

2 RELATED WORK

The process of assembling comminuted fracture is similar to repairing archeological findings, like pottery, chinaware, sculpture and monument. The main task is to find the correspondence and match them together. There are some studies which put forward methods helping to reassemble the fractured objects including semi-automatically and automatically.

2.1 Semi-automatic Methods

Papaioannou et al. [2] proposed a semi-automatic method dealing with archeological monuments. To avoid manual attempts with fragile and heavy fragments, they designed a system to assist archaeologists in reassembling monuments or smaller findings. They first construct 3D mesh from the pieces and segment them into faces. Parikh et al. [3] presented an approach in which the

user can easily reassemble an object from a large number of irrelevant pieces by iteratively picking correspondent parts. Mellado et al [4] presented a method based on a real-time interaction circle: an expert approximately points out initial relative orientations and positions between two fragments through an intuitive user interface. These initial poses are iteratively improved and corrected by the system in real time. Zhou et al. [1] proposed a for virtual reconstruction system for comminuted bone fractures. Users need to manipulate the fragment models and identify potential matches and then the alignment algorithms take the approximately placed fragments and find an arrangement that can minimize the global error of the alignment. Palmas et al. [5] proposed a computer-assisted constraint-based method for virtual reassembly of heritage works. The system involves users in the assembly process, digging their experience and professional knowledge. The core idea is to let users define how the fragments should be matched and then make use of all constraints.

However, these methods are not so intelligent, and need feedback from users to perform successive steps, which still calls for complicated manual work and professional experience. There

are some researchers going further to come up with some fully automatic methods.

2.2 Automatic Methods

The aim of automatic methods is to approximately compute initial position of every fragment through identifying corresponding feature among the fragments. Therefore, the key process is to choose a robust and expressive descriptor to represent the features of each fractured area. Shape descriptor that we need should be based on local features, which means it depends on the specific point as well as the neighborhood in certain radius and it won't be influenced by rigid transformation. Taking these prerequisites into account, the main task is similar to registration of 3D mesh or point set [6][7].

Huang et al [8] proposed a pipeline to resemble multiple fragments including segmentation, local registration and global registration. Segmentation is to identify fractured faces according to the roughness; local registration is pairwise matching of the pieces and construct a match graph to record the relationship between the candidates; global registration is to minimize the matching error and find an optimal solution. The framework is classical and widely adopted by others. Toler et al. [9] approach to determine matches between small pieces of artifacts like frescoes; they put forward a series of descriptors based not only on shape and color but also normal maps. Another work on computer-assisted matching of fragments is presented by Brown et al. [10] which is similar to the method of Koller et al. [11] who solved reconstructing of the Severan Marble Plan of ancient Rome. The method of McBride et al. [12] consists of two steps: they first compare each fragment pair and find similar parts of their boundaries by partial curve matching; then they seek for a globally optimal solution based on a best-first strategy so as to align pieces with the best match. Then a method base on hierarchical clusters of points matching is proposed by Winkelbach et al. [13]. It aims to combine two fragments and treat them as a new piece, and iteratively performs the matching process in a tree structure. What's better than others' approach is that when matching the larger piece, they simultaneously optimize the pairs already combined. Belenguer et al. [14] presented an automatic matching strategy using a shape-descriptor of a discrete sampling for the fracture surface. And then Zhang et al. [20] put forward new algorithm integrating fragments matching and template matching to reassemble thin-shell pieces, which performs effectively and robustly when reconstructing skulls and ceramic artifacts.

3 RECONSTRUCTION OF BONE MODEL

Medical CT is a diagnostic aid widely used by orthopedic doctors. CT tomography imaging reflects the attenuation rate of X-rays from different tissues. The reconstruction of three-dimensional models for medical two-dimensional images is a hot topic in medical data research. Some people tried to use AutoCAD

software to import CT images into a CAD window and create a three-dimensional model manually. However, the results of modeling have a certain difference with the actual situation, and it is difficult to meet medical requirements.

Materialise Mimics (Materialise's interactive medical image control system) is a medical image control system invented by Materialise. It is a modular structured software and can be configured according to different needs of users. It reads various scan data (CT, MRI), builds 3D models for editing, and then outputs widely used format like CAD, FEA, RP. Therefore, we perform the data conversing and processing works on Mimics Medical 20.0 and extra processing on Materialise 3-matic 11.0.

3.1 Importing CT Images

Run Mimics Medical 20.0, in the basic interface (Figure 3), enter File/Import Images, select the DIMCOM format file, and import, read a set of 16-slice spiral CT images. Four frames displayed views from different viewpoint of the image, with the upper left frame for front view, the lower left for side view, the upper right for top view and the lower right for perspective view. For any position of any view, we can use the mouse to directly click the position we want to operate. The position of the cross line will reach the clicked position. The other three views will also change accordingly.

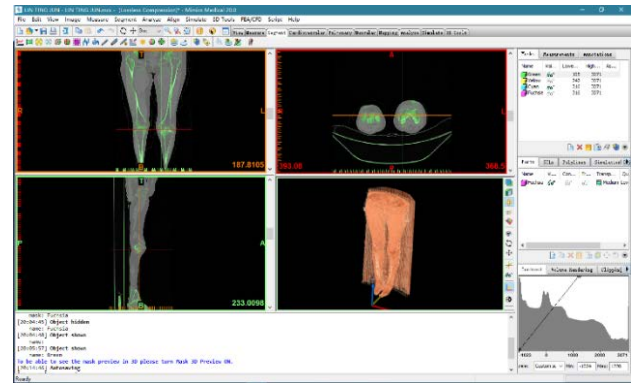


Figure 3: General interface of Mimics Medical 20.0

3.2 Separating Pieces

Due to the existence of soft tissue and precision limit of the scanning device, we may see the pieces are broken but still connect to each other. The connection can make negative effect to the final result, because the connected pieces can be seen as one object by the program and won't be processed. Therefore, we need to separate them before successive operation. The separating includes three steps:

- 1) Define a proper threshold to distinguish soft tissue and bones;
- 2) Use multiple slice edit to cut off invalid connection and make the contour clear;
- 3) Perform region growing algorithm to separate the piece.

The deciding of the threshold depends on the purpose of the model. It is easier to select the patient's soft tissue with a smaller threshold. If the threshold is larger, only the denser part will be retained. Enter segment tools in the menu bar and click thresholding (Figure 4). Choosing a proper upper and lower bound of threshold, we can get the image containing denser objects, which is almost bones.

However, they are still connected to each other by the cartilages and invalid areas. We can't remove the cartilage automatically because if the lower bound is set too low, some other tissue may be included which will cause more interference. We can only remove it manually. That's where multiple slice tool contributes. Click multiple slice edit in the segment menu, set proper parameter and take the brush to mark the area between two different bones (Figure 5). Scroll up and down to continue marking on different layers, and the tool can interpolate the interval between layers. Operate on different frames of view so that the bones can be totally separated.

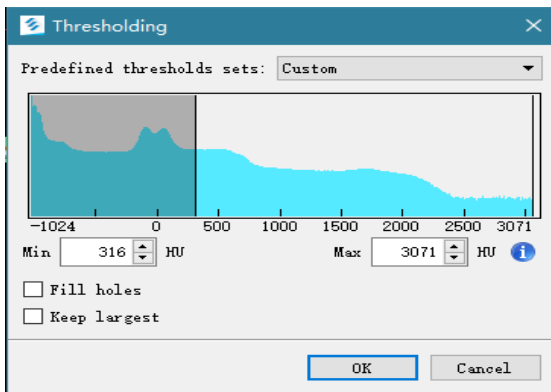


Figure 4: Set proper threshold

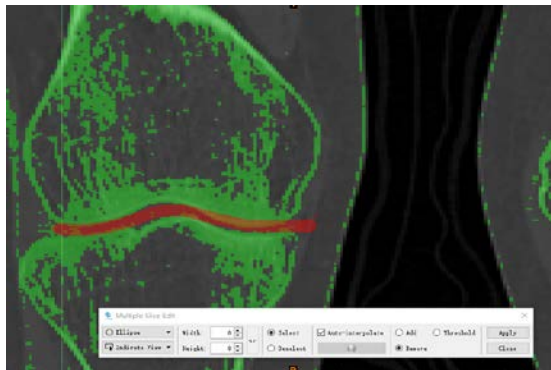


Figure 5: Mark the invalid connection

After multiple slicing, the bones are disconnected. Then we can perform the region growing to extract specific bone. Click the region growing tools in segment menu and choose the region we want to extract. If the region is totally isolated it will be selected alone (Figure 6).



Figure 6: Extracted bone (red region)

At last, we can export the extracted bone to Materialise 3-matic and perform some post processing. We can make modifications to on the model then smooth it to remove the noise. As the bone contains hollows and complex structures inside, it is inevitable for the model to hold some non-manifold or abnormal structures. We need clean it up and fix it in 3-matic. Finally, we get the 3D model we need.

4 CALCULATING KEYPOINTS AND DESCRIPTOR

Since the data size of our bone model is very large, it is computationally expensive as well as unnecessary to calculate local shape descriptor for every single point and match them directly. We should find some feature points that can reflect local feature around them.

4.1 Extracting Keypoints

Feature point detection is widely used in situations such as target matching, target tracking, and three-dimensional reconstruction. When modeling a targeted object, the target features are extracted from the model. Commonly used features include color, corner points, feature points, outlines, and textures. In the detection of feature points, the scale invariance, rotation invariance, and anti-noise effect are often proposed, which are indicators for determining whether the feature points are stable or not.

Desirable feature points must include but not limited to the following characteristics:

- 1) Reflecting real distinctive point in the model;
- 2) Accurate positioning performance;
- 3) High repetition rate of detection;
- 4) Robustness of noise;
- 5) High computational efficiency

According to the evaluation and comparison of some widely used detectors in the survey of Kang Tombari et al. [15], some fixed-scale detectors can be considered to extract keypoints, such

as Local Surface Patches (LSP) proposed by Chen and Bhanu [16], Intrinsic Shape Signatures (ISS) by Zhong [17], KeyPoint Quality (KPQ) by Mian et al. [18], Heat Kernel Signature (HKS) by Sun et al. [19]. These fixed scale detectors find different key points at a certain constant scale and provide it as a parameter of the algorithm. These detectors can be abstracted into two main steps. The main purpose of the initial optional step is to prune the input data by thresholding the quality metrics calculated for each point. Since great repeatability and efficiency are needed in rigid matching, we choose ISS to extract keypoints of our bone model.

In order to describe a local feature around a point which belongs to an object moving in global coordinates, it is a good way to create a local coordinate around this point, which makes sure the local coordinate system also rotates with the object. This is how ISS works. The covariance matrix of the adjacent regions of each 3D point is calculated first, and the points whose largest eigenvalues differs much with its second largest eigenvalues are designated as features. Obviously, the eigenvalues in this case are geometrically significant. The size of the eigenvalues is actually the length of the ellipsoidal axis. The shape of the ellipsoid is an abstract summary of the distribution of neighboring points. If the points are densely distributed in a certain direction, the direction will be the first main direction of the ellipsoid, the sparse direction is the second main direction, and the normal direction is the sparsest one (only one layer), naturally it is the third main direction.

As is shown in Figure 7, we extracted the keypoints of a fractured bone model using ISS algorithm. It marks distinctive points on the model and can represent the neighboring points.



Figure 7: Keypoints of a fractured bone model

4.2 Calculating Feature Descriptor

Keypoints are the most prominent points within certain range of local areas. To match a fragment with the template, we only need to find the correspondence of the keypoints respectively on the fragment and template. When two points are regarded as correspondent, it means that they are of the same position on the local coordinate and their neighboring structures are similar. Since it is hard to directly figure out the local position of a specific point,

comparing the neighboring structure becomes a feasible method. Therefore, we need a proper local feature descriptor.

To adapt to geometric diversity between the fragment and template, we prefer a descriptor that can reflect the distribution of points around the keypoints.

Spin image [21] counts distribution histogram of the neighboring points in the local cylindrical coordinate. The discrete process smooths the effect of each point by means of bilinear interpolation, and the descriptor has a certain anti-noise capability. The final spin image often needs a normalization step, which is obtained by dividing the maximum pixel value in the spin image. This step makes the spin map descriptor have a certain ability to resist changes in resolution. But the coordinate system is dependent on the normal vector of the feature points, which is prone to noise interference. And it does not consider the positional information of the field points, making the specificity lower.

3D shape context [22][23] extends from 2D shape context. It takes the normal vector of the feature point as the north pole of its spherical neighborhood, and then the regions are divided in the direction of radial, longitude, and latitude. Then the sum of the values of the weighted points that fall into each region is counted. But it performs poorly in the presence of background or noise.

In our work, we choose the SHOT (the Signature of Histograms of Orientations) descriptor [24][25], it is a robust and specific descriptor that combines geometric distribution information with histogram statistics. For the SHOT, LRF (local reference frame) is established based on the information of the feature point neighborhood. The spherical neighborhood of the feature points is divided into regions in the radial direction (inside and outside spheres), longitude (just like time zone), and latitude direction (south and north hemispheres) as Figure 8. In this way, the sphere is radially divided into two parts, longitude divided into eight, latitude is divided into two, thus 32 small areas in total.

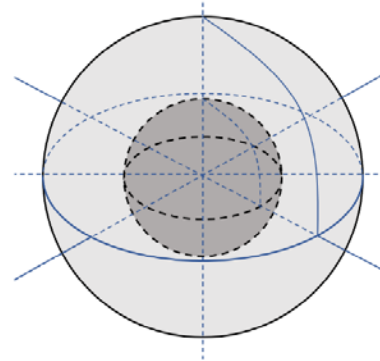


Figure 8: LRF (local reference frame)

The distribution of the cosine of the angle between the normal vector and the normal vector in each small area is calculated. The cosine value is divided into 11 bins (Figure. 9), so the length of SHOT descriptor is $32 \times 11 = 352$.

For each fragment F_i and template T , we respectively extract their keypoints and accordingly compute the descriptor $D(p), D(q)$, where $p \in F_i, q \in T$.

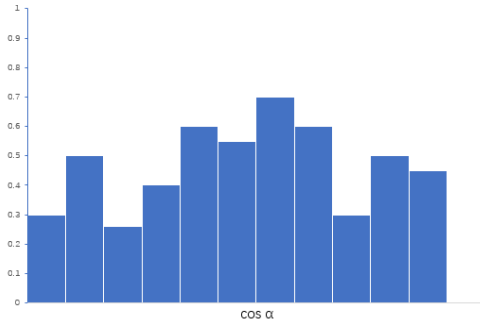


Figure 9: Distribution histogram

5 ALIGNING PIECES WITH TEMPLATE

Up to now, we have got the descriptor for all keypoints of fragments and template. Next, what we need to do is to find the correspondence between them. Specifically, for $p \in F_i, q \in T$, if

- 1) $\text{Dis}(p, q) = |D(p) - D(q)| < \delta_D$.
- 2) For a fixed $p, q \in T$ makes $\text{Dis}(p, q)$ smallest

then this pair (p, q) is seemed to be correspondent ($\delta_D = 0.05$ in our experiments), we add them into the match list M . As is shown in Figure 10, it may happen that some nonconforming pairs are added, because p and q are essentially 352-dimensional vectors, we simply match them according to mean quadratic deviation. Therefore, there needs to be a correspondence rejection. There are some effective refining methods like forward search [8], voting [26], graph matching [27], Since the size of set M is quite big and they will cause large amount of computation, we refer to RANSAC [28] instead. RANSAC stands for "RANdom SAmple Consensus". The input of this algorithm is a set of observations data (often containing large noise or inefficiency), a parametric model for interpretation of the observations, and some credible parameters. RANSAC achieves the goal by repeatedly selecting a set of random subsets in the data. Therefore, it has a certain probability to get a reasonable result, and in order to improve the probability, we must increase the number of iterations.

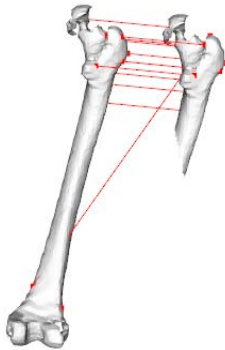


Figure 10: Mismatch of the keypoints

When refining the correspondence and aligning F_i with T , we randomly choose three pairs $(p_1, q_1), (p_2, q_2), (p_3, q_3) \in M$. As we only consider rigid transformation, we can accept these three pairs if the Euclidean distance between two points on F_i is similar to the parallel two points on T , namely

- 1) $|\|p_1 p_2\| - \|q_1 q_2\|| < \delta_p$
 - 2) $|\|p_2 p_3\| - \|q_2 q_3\|| < \delta_p$
 - 3) $|\|p_3 p_1\| - \|q_3 q_1\|| < \delta_p$
- ($\delta_p = 1mm$ in our experiments)

Through several iterations, we can find at least three pairs meeting our requirements. With the pairs, we need to estimate the transformation T_i for every fragment F_i . The transformation T_i is composed of translation t and rotation R . For each fragment, we calculate a pair of t and R to make the mean square error

$$e(F, T) = \sum_{i=0}^n (Rp_i + t - q_i)^2$$

as small as possible using SVD decomposition method. Finally, T_i is applied to each F_i so that fragments can be aligned with template.

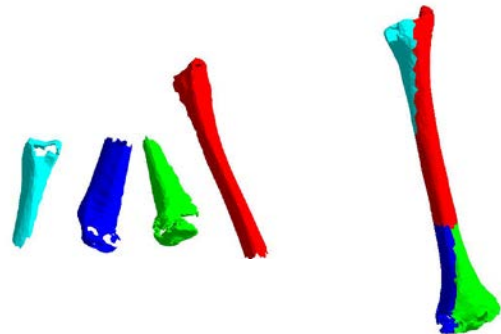
6 EXPERIMENTAL RESULTS

We designed a system to implement our method and examine it with series of CT data obtained by computed tomography scanner. The pipeline of our system is presented as Figure 2. For all the three cases, our system is able to reassemble the fragment and generate acceptable results. To evaluate the matching error, we define

$$\varepsilon = \frac{1}{n} \sum_{i=0}^n \|T(p_i) - q_i\|$$

($T(p_i)$ represents the point p_i applied transformation T)

We first tried a shin bone from a female patient and reconstruct the bone model from her CT data (Figure 11(1)). As we can see, the bone is broken into four parts including large fragments and tiny ones. We reassembled them with an error of $\varepsilon = 6.21$ (Figure 11(2)).



(1). fractured shin bone (2). reassembled shin bone

Figure 11

Then we worked on a thigh bone (as shown in Figure 12(1)), which comes from a female patient. The thigh bone is broken into five parts. Since the patient suffers from osteoporosis, the femoral head and lateral epicondyle are eroded, which may increase the level of difficulty. The body of femur is lack of prominent areas, so when extracting ISS keypoints we need to set the sample resolution lower to get as more keypoints as possible. The result is shown in Figure 12(2) and error $\epsilon = 6.89$.

To look for more challenges, we tried to reassemble a broken male cranial bone as shown in Figure 13(1). It contains various structures, making it harder to match the feature. Still, we managed to reassemble it with acceptable error as Figure 13(2).

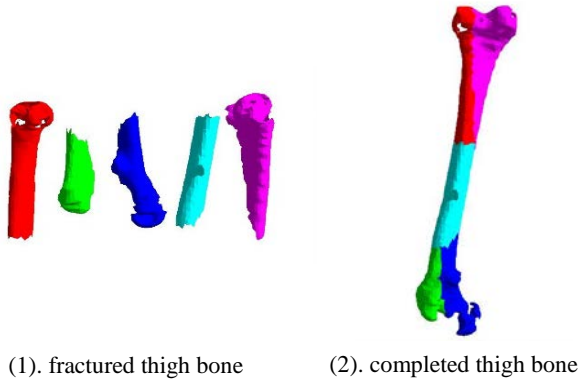


Figure 12

Our program is run on a PC with 2.7 GHz Core i5-6400 CPU and 8G RAM. The results of these three experiments are documented in the following table. **Nf** is the number of fragments, **Np** is the number of points, **Riss** is the radius of ISS (millimeter), **Rshot** is the radius of SHOT (millimeter), **Tiss** is the time of extracting keypoints (millisecond), **Tmatch** is the time of matching pieces (millisecond) and **E** is the matching error.

Bones	Nf	Np	Riss	Rshot	Tiss	Tmatch	E
shin	4	18642	1.5	5	12888	145362	6.21
thigh	5	24282	1.5	6	11518	376850	6.89
cranial	5	18216	1.8	5	18208	99931	2.41

To extract enough keypoints, we should set the radius of ISS relatively small. However, as the number of keypoints grows, it becomes more computationally complex to matching the features. Therefore, we need make tradeoff between them so that the computation process can be both effective and efficient.

Limitations. When the fragments become pretty small, the alignment results are not very satisfactory. In Figure 14, we try to align a small piece (containing 193 vertexes, 483 edges, 308 faces) of a thigh bone to the template. However, keypoints of the small piece are paired with keypoints located in two ends of the template, which is apparently incorrect.

As is mentioned above, feature descriptors reflect the local structure and points distribution around the keypoints through counting points and calculating angles in divided areas. When the scale of the piece becomes too small, it can't hold enough points and prominent features to identify itself.

This happens due to the lack of geometric information, which means it is hard to directly find a correspondent region on the template according to the shape. We can consider placing it after all the other fragments are properly arranged.

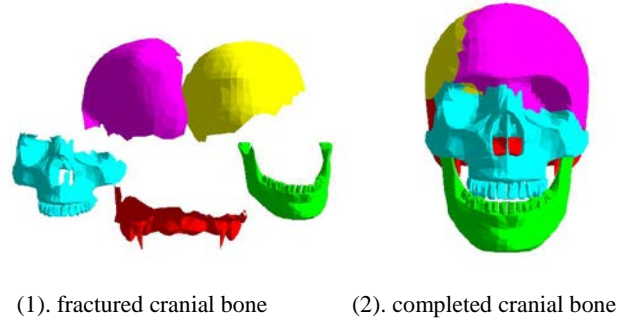


Figure 13

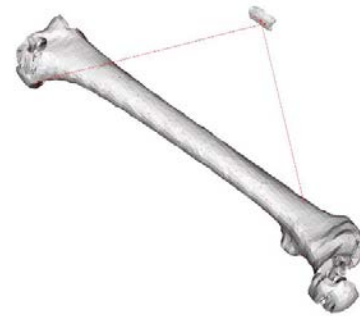


Figure 14: Aligning very small piece

7 CONCLUSION

This paper presents a complete pipeline of automatically reassembling fractured bones, which can provide some references to surgeon in orthopedic surgery. We introduce the way to create 3D model from CT image, extract the prominent points, analyze the structure and find correspondence among them. Through a series of experiments, our method is proved to be effective and robust in reassembling fractured bones while there are still limitations.

In the future, we expect to combine our system with the surgical restoration instrument. Our system computes the translation and rotation of each fragment and passes the transformation parameter to the instrument, so that the surgeon can obtain more help and further reduce the chance of making mistakes to lower the surgery risks.

ACKNOWLEDGEMENT

This study was supported by the National Natural Science Foundation of China (No.61872020, No.81601612) and Key Medical Subjects of Jiangsu Province (BE 2016763).

REFERENCES

- [1] Zhou, Beibei, et al. "Virtual 3D bone fracture reconstruction via inter-fragmentary surface alignment." international conference on computer vision, 2009: 1809-1816.
- [2] G. Papaioannou, E.-A. Karabassi, and T. Theoharis, "Virtual archaeologist: Assembling the past," IEEE Comput. Graph. and Appl., vol. 21, no. 2, Mar. 2001.
- [3] D. Parikh, R. Sukthankar, T. Chen, and M. Chen, "Feature-based Part Retrieval for Interactive 3D Reassembly," in Applications of Computer Vision, 2007. WACV'07. IEEE Workshop on. IEEE, 2007.
- [4] N. Mellado, P. Reuter, and C. Schlick, "Semi-automatic geometry-driven reassembly of fractured archeological objects," in Proc. VAST 2010. Eurographics, 2010, pp. 33–38.
- [5] Palmas, G, et al. "A computer-assisted constraint-based system for assembling fragmented objects." Digital Heritage International Congress IEEE, 2013:529-536.
- [6] H. Pottmann, S. Leopoldseder, and M. Hofer, "Simultaneous registration of multiple views of a 3d object," in Intl. Archives of the Photogram-metry, Remote Sensing and Spatial Information Sciences, Vol. XXXIV, Part 3A, Commission III, 2002, pp. 265–270.
- [7] Krishnan S, Lee P Y, Moore J B, et al. Global registration of multiple 3D point sets via optimization-on-a-manifold[C]. symposium on geometry processing, 2005: 187-196.
- [8] Q.-X. Huang, S. Flori, N. Gelfand, M. Hofer, and H. Pottmann, "Reassembling fractured objects by geometric matching," ACM Transactions on Graphics, vol. 25, no. 3, Jul. 2006.
- [9] C. Toler-Franklin, B. Brown, T. Weyrich, T. Funkhouser, S.Rusinkiewicz, and D. Texture, "Multi-Feature Matching of Fresco Fragments," ACM Transactions on Graphics (TOG), vol. 29, no. 6, 2010.
- [10] B. J. Brown, L. Laken, P. Dutré, L. V. Gool, S. Rusinkiewicz, and T. Weyrich, "Tools for virtual reassembly of fresco fragments," in International Conference on Science and Technology in Archaeology and Conservations, Dec. 2010.
- [11] D. R. Koller, "Virtual archaeology and computer-aided reconstruction of the severan marple plan," in Beyond Illustration: 2D and 3D Digital Technologies as Tools for Discovery in Archaeology British Archaeological Reports International Series. Archaeopress, 2008, pp. 125–134.
- [12] J. C. McBride and B. B. Kimia, "Archaeological Fragment Reconstruction Using Curve-Matching," in 2003 Conference on Computer Vision and Pattern Recognition Workshop. Ieee, Jun. 2003.
- [13] S. Winkelbach and F. M. Wahl, "Pairwise matching of 3d fragments using cluster trees," Int. J. Comput. Vision, vol. 78, no. 1, pp. 1–13, Jun. 2008.
- [14] C. Sanchez-Belenguer and E.Vendrell-Vidal, "Archaeological fragment characterization and 3d reconstruction based on projective gpu depth maps," in Virtual Systems and Multimedia (VSMM), 2012 18th Inter-national Conference on, 2012, pp. 275–282.
- [15] F. Tombari, S. Salti, and L. DiStefano. Performance evaluation of 3d keypoint detectors. International Journal of Computer Vision, 102(1-3):198–220, 2013
- [16] Chen H, Bhanu B. 3D free-form object recognition in range images using local surface patches[C]. international conference on pattern recognition, 2004: 136-139.
- [17] Zhong Y. Intrinsic shape signatures: A shape descriptor for 3D object recognition[C]. international conference on computer vision, 2009: 689-696.
- [18] Mian A S, Bennamoun M, Owens R, et al. On the Repeatability and Quality of Keypoints for Local Feature-based 3D Object Retrieval from Cluttered Scenes[J]. International Journal of Computer Vision, 2010: 348-361.
- [19] Sun J, Ovsjanikov M, Guibas L J, et al. A concise and provably informative multi-scale signature based on heat diffusion[J]. symposium on geometry processing, 2009, 28(5): 1383-1392.
- [20] Zhang K, Yu W, Manhein M H, et al. 3D Fragment Reassembly Using Integrated Template Guidance and Fracture-Region Matching[C]. international conference on computer vision, 2015: 2138-2146.
- [21] A. Johnson and M. Hebert. Using spin images for efficient object recognition in cluttered 3d scenes. PAMI, IEEE Trans. on, 21(5):433–449, 1999.
- [22] Tombari F, Salti S, Stefano L D, et al. Unique signatures of histograms for local surface description[C]. european conference on computer vision, 2010: 356-369.
- [23] S. Belongie, J. Malik, and J. Puzicha. Shape matching and object recognition using shape contexts. PAMI, IEEE Trans. on, 24(4):509–522, 2002.
- [24] F. Tombari, S. Salti, and L. Di Stefano. Unique signatures of histograms for local surface description. In Proc. of the 11th ECCV: Part III, pages 356–369, 2010.
- [25] Salti S, Tombari F, Stefano L D, et al. SHOT: Unique signatures of histograms for surface and texture description[J]. Computer Vision and Image Understanding, 2014: 251-264.
- [26] D. G. Lowe. Distinctive image features from scale-invariant keypoints. Int. J. Comput. Vision, 60(2):91–110, 2004.
- [27] D. Conte, P. Foggia, C. Sansone, and M. Vento. Thirty years of graph matching in pattern recognition. International journal of pattern recognition and artificial intelligence, 18(03):265–298, 2004.
- [28] Fischler M A, Bolles R C. Random sample consensus: a paradigm for model fitting with applications to image analysis and automated cartography[J]. Communications of The ACM, 1981, 24(6): 381-395.